Full-Wave Modal Analysis of Arbitrarily-Shaped Dielectric Waveguides Through an Efficient Boundary-Element-Method Formulation

Carlo Di Nallo, *Student Member, IEEE*, Fabrizio Frezza, *Member, IEEE*, and Alessandro Galli, *Student Member, IEEE*

Abstract— **In this work an original procedure, based on the boundary element method (BEM), is carried out for the full-wave modal analysis of dielectric waveguiding structures with arbitrary cross section. A novel integral-equation formulation is developed after a careful analysis of the discontinuities in the dyadic kernel. Numerical solutions are then achieved and tested for both conventional and the new algorithms. Results for several important practical structures are obtained and compared to data from other numerical approaches and from measurements, to emphasize the accuracy, efficiency, and versatility of the new implementation.**

I. Introduction

THE ELECTROMAGNETIC characterization of dielectric waveguiding structures is an area of considerable theoretical and practical interest, both for microwave and for optical applications [1], [2]. Many different types of dielectric guides have been the subject of several analysis techniques. Since most of these structures cannot be solved analytically, various numerical methods have been previously developed in order to calculate the relevant modal properties (propagation wavenumbers, field configurations, etc.). In the literature, a lot of material can be found about these numerical methods and the distinctive computational features (accuracy, versatility, efficiency, and so forth) [3], [4].

In this work, a new procedure is developed based on the boundary element method (BEM), and used to solve the modal problem for cylindrical dielectric structures having arbitrary cross section. The new method is accurate, efficient, and gives complete information about the guiding structures.

As is well known, the complexity reduction of one spatial dimension, typical of BEM approaches, is extremely convenient in terms of memory space and computation time [4]; on the other hand, problems can arise from rather involved pre-processing, and numerical convergence.

Compared with the BEM formulations already outlined in the literature [5]–[7], the procedure that is developed here has some important distinctive advantages. In particular, with the present formulation it is possible to have great flexibility in the choice of basis functions for the unknowns, thus enlarging significantly the class of algorithms for the numerical solution of the integral equations. To achieve this, and to eliminate some complicated numerical problems, a detailed analysis of the singularities of the integral-equation kernels (represented by dyadic Green's functions) becomes necessary. The numerical solution is then obtained through different discretization techniques, both usual (point matching and Galerkin's methods [4], [6]) and unusual (Nystrom method [8]), which are tested as for their accuracy and efficiency.

This BEM procedure provides a new competitive tool for full-wave modal analysis of a variety of dielectric structures of practical interest. Several examples are simulated here, including both uniform dielectric waveguides and resonators of NRD (nonradiative dielectric) type [9], having various common and uncommon shapes. Specific attention is paid to problems that are extremely sensitive from a computational viewpoint: for instance, the effects of slight perturbations in the cross section shape (e.g., notches or cuts) are tested, thus deriving useful information for the design of devices such as filters of dual-mode type [10].

Our results are compared to data from various numerical techniques presented in the literature [11]–[15]; other useful information is derived by developing specific reference methods and comparing with experimental investigations [9, 10]. These tests demonstrate the important qualities of this new BEM approach, emphasizing the excellent properties of accuracy, economy and versatility.

II. Description of the Analysis Procedure

The boundary element method is applied here with the goal of obtaining the complete spectrum of guided modes for cylindrical dielectric structures of arbitrary cross section, as shown in Fig. 1.

The general formulation of the problem is based on the equivalence principle, by expressing the fields in the interior and exterior of the cylinder by means of free-space dyadic Green's functions, related to the different media which occupy the two regions. By imposing the continuity of the unknown tangential components of the electric and magnetic fields on the air/dielectric interface, a coupled set of integral equations on the interface surface is obtained.

According to the standard approaches, the longitudinal symmetry shown by the structures of interest suggests a common z-dependence of the type $\exp(-j\beta z)$ for the unknowns, where β is the propagation constant. The integration along z furnishes a Fourier transform and the problem becomes two-

Manuscript received March 7, 1995; revised July 10, 1995.

The authors are with "La Sapienza" University of Rome, Italy, Department of Electronic Engineering, 00184 Rome, Italy.

IEEE Log Number 9415454.

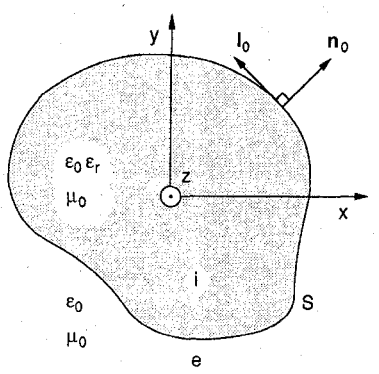

Fig. 1. Cylindrical dielectric waveguide structure of arbitrary cross section, analyzed with the boundary element method (BEM). The local coordinate system on the boundary and the other parameters introduced in the analysis are indicated.

dimensional. In the cross section of the structure the position vector will be represented by $\mathbf{r}_t$; on the boundary s of the cross section (where the integrations are performed), a local rectangular coordinate system $\mathbf{n}_0, \mathrm{l}_0, \mathbf{z}_0$ (normal, tangential, and longitudinal unit vectors, respectively) may be chosen, as shown in Fig. 1.

The fields in the external (superscript e) and internal (superscript i) regions can be expressed in the following integral forms (we present for brevity only the expression for the electric field, since it is possible to immediately deduce the magnetic field by means of the duality principle)

$$\begin{aligned}\mathbf{E}^{e/i}(\mathbf{r}_t) = &-/+ j\omega\mu_0 \oint_s \mathbf{J}_e(\mathbf{r}'_t)\cdot\bar{\mathbf{G}}_t^{e/i}(\mathbf{r}'_t,\mathbf{r}_t;\beta)ds' \\ &-/+\oint_s \mathbf{J}_m(\mathbf{r}'_t)\cdot(\nabla'_t + j\beta\mathbf{z}_0) \\ &\times \bar{\mathbf{G}}_t^{e/i}(\mathbf{r}'_t,\mathbf{r}_t;\beta)ds' \end{aligned} \tag{1}$$

where the equivalent electric and magnetic currents $\mathbf{J}_e$ and $\mathbf{J}_m$ are defined as

$$\begin{aligned}\mathbf{J}_e &= \mathbf{n}_0\times\mathbf{H} = \mathbf{z}_0 H_l - \mathrm{l}_0 H_z = \mathbf{z}_0 J_{ez} - \mathrm{l}_0 H_z \\ \mathbf{J}_m &= -\mathbf{n}_0\times\mathbf{E} = -\mathbf{z}_0 E_l + \mathrm{l}_0 E_z = \mathbf{z}_0 J_{mz} + \mathrm{l}_0 E_z\end{aligned} \tag{2}$$

and the transformed free-space dyadic Green's functions $\bar{\mathbf{G}}_t^{e/i}$ are deduced from the two-dimensional scalar Green's function g_t

$$\begin{aligned}\bar{\mathbf{G}}_t^{e/i}(\mathbf{r}'_t,\mathbf{r}_t;\beta) &= \left[\bar{\mathbf{I}} + \frac{1}{k^2}(\nabla'_t + j\beta\mathbf{z}_0)(\nabla'_t + j\beta\mathbf{z}_0)\right] \\ &\quad\times g_t^{e/i}(\mathbf{r}'_t,\mathbf{r}_t) \\ g_t^e(\mathbf{r}'_t,\mathbf{r}_t) &= \frac{1}{4j}H_0^{(2)}(k_{t0}|\mathbf{r}'_t - \mathbf{r}_t|), \\ g_t^i(\mathbf{r}'_t,\mathbf{r}_t) &= \frac{1}{4j}H_0^{(2)}(k_{t\varepsilon}|\mathbf{r}'_t - \mathbf{r}_t|)\end{aligned} \tag{3}$$

where: $k_{t0}^2 = k_0^2 - \beta^2$, $k_{t\varepsilon}^2 = k_0^2\varepsilon_r - \beta^2$, and k is the wavenumber of the medium in which the corresponding Green's function is calculated: i.e., $k = k_0 = \omega\sqrt{\mu_0\varepsilon_0}$ in the air (e region) and $k = k_0\sqrt{\varepsilon_r}$ in the dielectric (i region).

In spite of the relative simplicity of the BEM formulation, the effective solution of the integral-equation system presents considerable difficulties, both from the analytical and the numerical point of view.

In connection with these questions, it should be pointed out that in the BEM procedure presented in the literature [5]–[7] the operations involving derivatives on the Green's functions are usually transferred to the unknowns, so that the degree of singularity for the integral kernels is reduced. In the present formulation, however, we have preferred to maintain the derivative operations on the Green's functions, in order to make the choice of basis functions in the expansion of the unknowns more flexible. As a consequence, this choice allows us to significantly enlarge the class of the numerical techniques that can be used for faster and more accurate solutions (this point is discussed in detail in the next section).

The advantages of such a formulation require, in contrast, a large amount of analytical processing: in particular, a specific attention has to be paid in evaluating the influence of the kernel's singularities, as the degree of singularity is no longer reduced. Since the dyadic Green's functions diverge when the source and the observation points coincide on the boundary s, the integrals have to be evaluated in the limit for which the observation point tends to the boundary from the appropriate (external or internal) region.

If the boundary s is assumed to be represented as a polygonal contour, this limit procedure can be applied in a rigorous way: it leads to suitable expressions for the external and internal electromagnetic fields, which are represented by the sum of various terms

$$\begin{aligned}\frac{1}{2}\mathbf{E}^{e/i}(\mathbf{r}_t) = &-/+\oint_s J_{mz}(\mathbf{r}'_t)\left(\frac{\partial}{\partial n'}g_t^{e/i}\mathrm{l}'_0 - \frac{\partial}{\partial l'}g_t^{e/i}\mathbf{n}'_0\right)ds' \\ &-/+\oint_s E_z(\mathbf{r}'_t)\left(-\frac{\partial}{\partial n'}g_t^{e/i}\mathbf{z}_0 + j\beta g_t^{e/i}\mathbf{n}'_0\right)ds' \\ &-/+\frac{j\omega\mu_0}{k^2}\oint_s J_{ez}(\mathbf{r}'_t)\left(j\beta\frac{\partial}{\partial n'}g_t^{e/i}\mathbf{n}'_0\right. \\ &\left.+ j\beta\frac{\partial}{\partial l'}g_t^{e/i}\mathrm{l}'_0 + k^2 g_t^{e/i}\mathbf{z}_0 - \beta^2 g_t^{e/i}\mathbf{z}_0\right)ds' \\ &+/-\frac{j\omega\mu_0}{k^2}\oint_s H_z(\mathbf{r}'_t)\left(\frac{\partial^2}{\partial n'\partial l'}g_t^{e/i}\mathbf{n}'_0\right. \\ &\left.+ k^2 g_t^{e/i}\mathrm{l}'_0 + j\beta\frac{\partial}{\partial l'}g_t^{e/i}\mathbf{z}_0\right)ds' \\ &+/-\frac{j\omega\mu_0}{k^2}\oint_s H_z(\mathbf{r}'_t)\frac{\partial^2}{\partial l'^2}g_t^{e/i}\mathrm{l}'_0\,ds'.\end{aligned} \tag{4}$$

The last term of the previous expression diverges when the observation point lies on the boundary, and requires a "finite part" integral operation in order to be evaluated numerically [6]. To overcome such a difficulty, it is observed that the second derivative with respect to the tangential coordinate of the scalar Green's function g_t presents a singular behavior that does not depend on the characteristics of the media; therefore, this singularity can be eliminated by suitably combining the expressions for the interior and exterior fields. Because of the presence of the factor $1/k^2$ before the last integral term, this simplification can be accomplished by multiplying the interior field by ε_r and adding the resulting expression to the exterior

field. For the magnetic-field equation analogous considerations can be applied.

Performing this simplification, and assuming the continuity of the tangential fields, we have reached the following fundamental expression for the integral-equation system, from which the numerical solution has been derived

$$\begin{aligned}
&\frac{\left\{\begin{matrix}\varepsilon_r\\1\end{matrix}\right\}+1}{2}\mathbf{n}_0\times\left\{\begin{matrix}\mathbf{E}(\mathbf{r}_t)\\\mathbf{H}(\mathbf{r}_t)\end{matrix}\right\}\\
&+\mathbf{n}_0\left\{\oint_s\left\{\begin{matrix}\mathbf{J}_{mz}(\mathbf{r}'_t)\\-\mathbf{J}_{ez}(\mathbf{r}'_t)\end{matrix}\right\}\left[\frac{\partial}{\partial n'}\left(g_t^e-\left\{\begin{matrix}\varepsilon_r\\1\end{matrix}\right\}g_t^i\right)\mathbf{l}'_0\right.\right.\\
&\qquad\left.\left.-\frac{\partial}{\partial l'}\left(g_t^e-\left\{\begin{matrix}\varepsilon_r\\1\end{matrix}\right\}g_t^i\right)\mathbf{n}'_0\right]ds'\right.\\
&+\oint_s\left\{\begin{matrix}E_z(\mathbf{r}'_t)\\H_z(\mathbf{r}'_t)\end{matrix}\right\}\left[-\frac{\partial}{\partial n'}\left(g_t^e-\left\{\begin{matrix}\varepsilon_r\\1\end{matrix}\right\}g_t^i\right)\mathbf{z}_0\right.\\
&\qquad\left.+j\beta\left(g_t^e-\left\{\begin{matrix}\varepsilon_r\\1\end{matrix}\right\}g_t^i\right)\mathbf{n}'_0\right]ds'\\
&+j\omega\left\{\begin{matrix}\mu_0\\\varepsilon_0\end{matrix}\right\}\oint_s\left\{\begin{matrix}\mathbf{J}_{ez}(\mathbf{r}'_t)\\\mathbf{J}_{mz}(\mathbf{r}'_t)\end{matrix}\right\}\\
&\times\left[j\frac{\beta}{k_0^2}\frac{\partial}{\partial n'}(g_t^e-g_t^i)\mathbf{n}'_0+j\frac{\beta}{k_0^2}\frac{\partial}{\partial l'}(g_t^e-g_t^i)\mathbf{l}'_0\right.\\
&\quad\left.+(g_t^e-\varepsilon_r g_t^i)\mathbf{z}_0-\frac{\beta^2}{k_0^2}(g_t^e-g_t^i)\mathbf{z}_0\right]ds'\\
&-j\omega\left\{\begin{matrix}\mu_0\\\varepsilon_0\end{matrix}\right\}\oint_s\left\{\begin{matrix}H_z(\mathbf{r}'_t)\\-E_z(\mathbf{r}'_t)\end{matrix}\right\}\\
&\times\left[\frac{1}{k_0^2}\frac{\partial^2}{\partial n'\partial l'}(g_t^e-g_t^i)\mathbf{n}'_0+(g_t^e-\varepsilon_r g_t^i)\mathbf{l}'_0\right.\\
&\quad\left.+j\frac{\beta}{k_0^2}\frac{\partial}{\partial l'}(g_t^e-g_t^i)\mathbf{z}_0\right]ds'\\
&-j\omega\left\{\begin{matrix}\mu_0\\\varepsilon_0\end{matrix}\right\}\oint_s\left\{\begin{matrix}H_z(\mathbf{r}'_t)\\-E_z(\mathbf{r}'_t)\end{matrix}\right\}\frac{1}{k_0^2}\frac{\partial^2}{\partial l'^2}(g_t^e-g_t^i)\mathbf{l}'_0ds'\Bigg\}=0.
\end{aligned}\tag{5}$$

All the terms of this pair of equations can be evaluated numerically everywhere, except for a neighborhood of the observation point, where some of the terms in (5) involving tangential derivatives have to be evaluated as Cauchy's principal integrals.

III. Procedures for the Numerical Solution

The integral equation expression that has here been obtained describes rigorously the electromagnetic eigenvalue problem for any dielectric waveguiding structure whose contour can be reduced to a polygon. As previously discussed, the present formulation permits us to enlarge and improve the numerical techniques for the solution.

A. Moment-Method Approach

By following the most common approach known in the literature, the coupled integral equation system has first been solved using the method of moments (MoM) [4], [6]. Since the derivative operations on the unknowns have been intentionally avoided in this approach, the most effective choice for their expansion appears to be the linear combination of basis functions that are piecewise constant. In this case the expansion allows us to perform analytical integrations without approximations in the neighborhood of the observation points.

The easiest way to perform the testing is by point matching, in which the continuity of the tangential components is enforced at a number of points (chosen in the middle of each integration subinterval) equal to the number of basis functions used in the expressions of the unknowns.

A solution has also been developed with Galerkin's method, where the testing functions are equal to the basis functions. This requires a double integration which may be performed using standard numerical techniques (Gaussian integration) [8].

The computational properties of the MoM implementations have generally appeared quite satisfactory. Our integral equation formulation, however, allows us to significantly enrich the class of available numerical techniques through the implementation of another attractive approach, which is presented next.

B. Nystrom Method

In addition to the MoM approaches, we have also carried out an interesting alternative procedure, which is not applicable to the formulations already known in the literature, since the absence of derivative operations on the unknown functions is expressly required. This procedure consists of a suitable adaptation of an integral equation solution method, often referred to as Nystrom method [8], based on quadrature formulas. The basic lines of the procedure are here explained.

Let us consider, with the sole object of simplifying the notation, a scalar form of the integral equations system (5), that can be presented in the following way

$$f(r)=\int_a^b K(r,r')f(r')\,dr'.\tag{6}$$

We can formally carry out a numerical integration of the previous relation by using a suitable quadrature rule with weights w_j, thus obtaining an approximate expression for the unknown function f

$$f(r)=\int_a^b K(r,r')f(r')dr'\cong\sum_{j=1}^{N}w_jK(r,r'_j)f(r'_j).\tag{7}$$

By forcing the previous relation to be exactly satisfied at the N quadrature abscissas ($r=r'_j$), one obtains a matrix equation for the values of the unknown function f in the finite number N of points.

This procedure, which is quite simple in principle, is not directly applicable to (5), because it corresponds to the case in which the kernel K becomes infinite when $r=r'_j$. However, if the kernel is integrable, as it is in the system (5), the Nystrom approach may still be applied, after a rearrangement of the integral equation(6) into the following equivalent form

$$f(r)=\int_a^b K(r,r')[f(r')-f(r)]\,dr'+f(r)\int_a^b K(r,r')\,dr'.\tag{8}$$

The argument of the first integral is no longer singular when $r = r'$ but assumes in this case a null value. The second integral involves only the kernel K, which is assumed integrable, and can thus be evaluated analytically or numerically.

From expression (8), the following linear approximating system is derived, which can be adapted to solve the original integral equation (6)

$$f(r_i) = \sum_{j=1}^{N} w_j K(r_i, r_j)[f(r_j) - f(r_i)] + f(r_i)R(r_i)], \qquad i = 1, 2, \ldots, N \quad (9)$$

where we have set

$$R(r_i) = \int_a^b K(r_i, r')\, dr'. \quad (10)$$

Fundamental advantages derive from the Nystrom formulation, specifically due to the fact that no set of basis functions is required for the unknowns and also numerical integrations on the boundary are avoided. Suitable tests and comparisons have demonstrated that the Nystrom method, by virtue of these properties, generally possesses characteristics of calculation speed and accuracy superior than MoM.

Moreover, it should be noted that expression (9) furnishes an optimal interpolation formula for calculating the unknown functions at points which do not coincide with the quadrature ones (by replacing r_i with arbitrary r). Further advantageous features of the Nystrom method will be discussed in the following sections.

C. Implementation of the Numerical Solution

As is typical for this kind of problems, once a homogeneous linear system of equations is obtained through the discretization operations, the eigensolutions for the electromagnetic field are derived by enforcing the condition that the determinant of the coefficient matrix is zero. From a numerical standpoint, the location of these zeros is an ill-conditioned problem. Reliable results have here been obtained by evaluating nearly null minima of the squared modulus of the determinant, thus avoiding the very delicate numerical search for complex zeros.

Alternatively, the same degree of accuracy can be achieved by searching for the null minima of the amplitudes of the matrix eigenvalues; this method requires a greater computational effort, but enables us both to distinguish between degenerate solutions and to evaluate the field behavior through the calculation of the relevant eigenvectors.

The convergence properties of the described algorithms have generally appeared quite satisfactory. This allows us to achieve sufficiently accurate results even though the matrix dimensions are kept rather small. Consequently, in particular with Nystrom implementation, the computation times are extremely reduced in comparison with other typical numerical techniques (FEM, mode matching, etc.). Further information on the peculiarities of the method will be provided in the next section.

IV. Results and Discussion

The above described procedure enables us to determine the propagation characteristics, the field configurations, etc.,

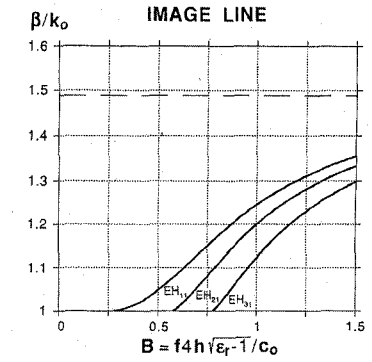

(a)

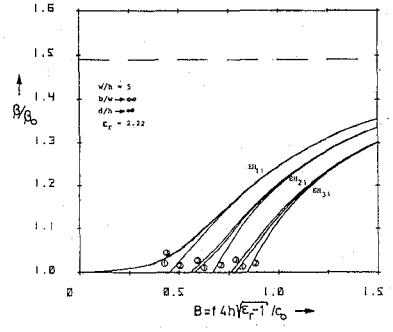

(b)

Fig. 2. (a) BEM dispersion curves (β/k_0 versus $B = f4h\sqrt{\varepsilon_r - 1}/c_0$) for the lowest modes of an image line (width $2w$, height h) using the choice of parameters given in Fig. 11 of [11]; (b) reference results given in Fig. 11 of [11]. Parameters $\varepsilon_r = 2.22; w/h = 5$.

for a full-wave modal analysis of arbitrarily-shaped dielectric waveguides.

Various tests have here been carried out both for guiding dielectric structures already known in the literature and also for dielectric resonators that find novel interesting applications. All the BEM data that will now be presented are derived with the Nystrom approach, due to its better performance. On the basis of such tests, a discussion of the distinctive features of this numerical formulation may be outlined.

A. Results for Dielectric Waveguides

In the literature, a great number of dielectric waveguides have been tested through various numerical methods (among the most common: finite-element, finite-difference, mode-matching, and integral-equation methods). Referring to some of the available data, we present and compare here results for a variety of geometries investigated with BEM.

As a first example, we consider the image line [11], which, as is well-known, is not solvable analytically. Various techniques have been employed, some of which are derivable from the approaches used for rectangular-section dielectric waveguides [12], [13]. The case shown in Fig. 2(a) gives the modal dispersion curves from BEM for the first modes of an image line, with the same choice of parameters as presented in [11]: direct comparisons are possible with the various methods reported specifically in Fig. 11 of [11], illustrated separately in Fig. 2(b) for the sake of clarity (the same normalized variables

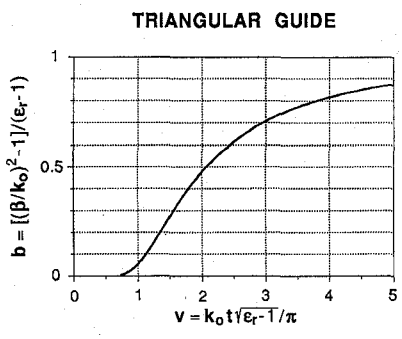

(a)

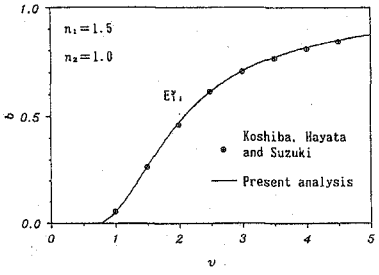

(b)

Fig. 3. (a) BEM dispersion curves ($b = [(\beta/k_0)^2 - 1]/(\varepsilon_r - 1)$ versus $v = k_0 t\sqrt{\varepsilon_r - 1}/\pi$) for the first mode of an equilateral triangular dielectric waveguide of height t, according to the choice of parameters given in Fig. 7(b) of [14]; (b) reference results given in Fig. 7(b) of [14]. Parameters: $\varepsilon_r = 2.25$.

and plot dimensions in [11] have been chosen). Additional results for structures having rectangular cross section will be provided in the next section for parallelepiped resonators.

Another dielectric-waveguide geometry tested here, which may present numerical difficulties due to sharp edges, is the triangular-section guide. The results for the dispersion curves of the first mode of an equilateral-triangle guide (of height t) shown in Fig. 3(a) may be compared for instance with the analogous situation in Fig. 7(b) of [14], which shows some different approaches: this is shown separately in Fig. 3(b) (again with the same normalized variables and plot dimensions as in the reference, to facilitate the comparisons).

Other specific cross sectional shapes have been analyzed, and further results will now be reported for these using NRD dielectric resonators instead of uniform waveguides, exploiting an additional way of comparing numerical results.

B. Results for Dielectric Resonators

The BEM procedure can easily be extended to compute the resonant frequencies of resonators of NRD type [9]. In fact, these NRD resonators can be viewed as sections of dielectric waveguides that are short-circuited by two (infinite) parallel metal plates, placed perpendicularly to the longitudinal axis at a certain distance a apart (usually chosen less than half the free-space wavelength). In Fig. 4 we show the most usual types of NRD resonators, with the relevant parameters: a disc (or circular-section) and a parallelepiped (or rectangular-section) NRD resonator in Fig. 4(a), and a notched square-section resonator in Fig. 4(b) (discussed further later). For these resonators, the β value is fixed by the presence of the

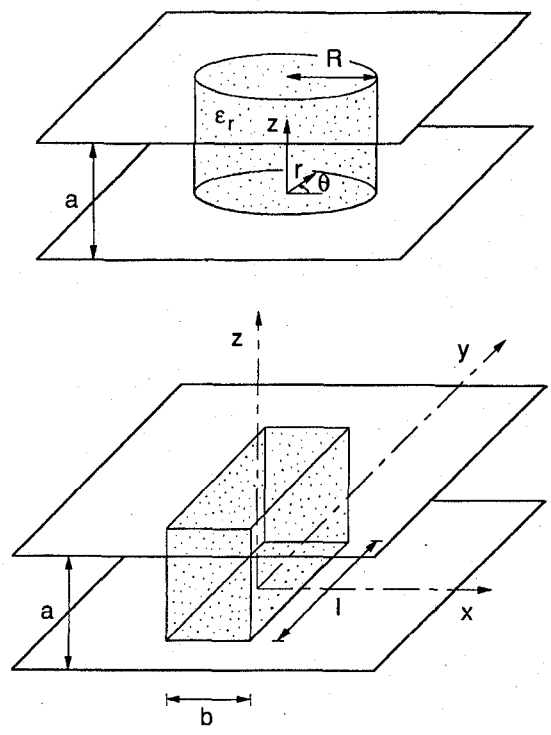

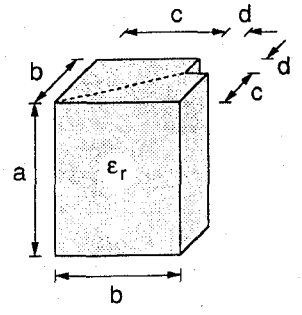

Fig. 4. Typical nonradiative dielectric (NRD) resonators, which can be viewed as sections of dielectric waveguides sandwiched between infinite metal plates at a distance a apart, perpendicular to the axis direction; the geometrical parameters and the coordinate systems are also indicated: (top) disc with radius R (upper) and parallelepiped with transverse dimensions b and l (lower). (Bottom) a notched square-section resonator (shown without the plates) with unperturbed sides b, notched sides c, and symmetrical corner's cuts of amplitude $d(b = c + d)$. Modes show perfect-electric-wall (PEW) and perfect-magnetic-wall (PMW) symmetries with respect to the minor diagonal, dashed in the figure.

plates ($\beta = m\pi/a$, with integer m), and the solution of the integral-equation system is possible only at discrete resonance frequencies.

Different examples have been considered here for typical NRD components in order to verify in a straightforward manner (including comparisons with experiments) the accuracy of the described method.

A first class of examples concerns dielectric structures with rectangular cross section (transverse dimensions b and l). In Fig. 5 we show a mode chart for the resonant frequencies f as

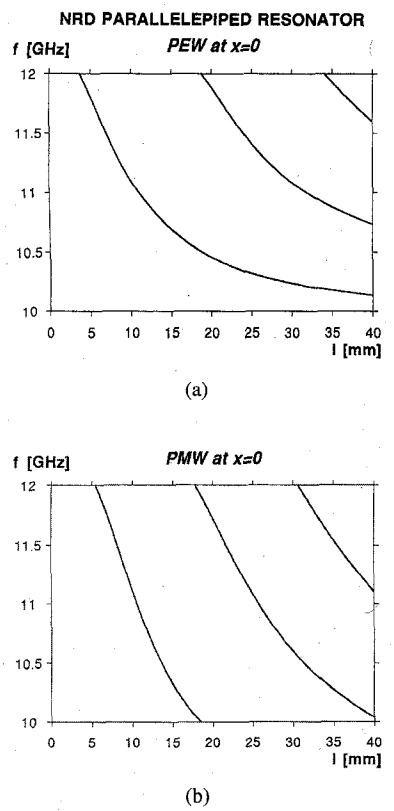

Fig. 5. BEM results for the frequencies f of the resonant modes as functions of the length l for rexolite NRD rectangular-section resonators of width b and height a: (a) insertion of a longitudinal PEW at $x = 0$; (b) insertion of a longitudinal PMW at $x = 0$. Parameters: $\varepsilon_r = 2.53; a = 12.3$ mm; $b = 10.15$ mm.

functions of the length l of parallelepiped NRD resonators, for a fixed choice of the other parameters (defined in Fig. 4(a)). A half-sinusoid vertical (z) variation of the fields is assumed, as is customary in NRD devices. The symmetrical cases corresponding to either a perfect electric or a perfect magnetic wall (PEW or PMW) placed centrally and parallel to the l sides (i.e., on the yz plane at $x = 0$), are plotted in Fig. 5(a) and (b), respectively. For these cases, it has been possible to make comparisons both with measured values (derived by an X-band NRD-guide experimental setup, with prototypes made from rexolite ($\varepsilon_r = 2.53$)) and with theoretical values (obtained from alternative techniques, such as finite elements, point matching, and approximated transverse resonance) [9]. Some numerical data are presented in Table I for the PEW case shown in Fig. 5(a).

As previously mentioned, in addition to the modal eigensolutions, the BEM method also enables a direct computation of the unknown equivalent currents (defined in (2)) on the surface s, and also of the electromagnetic field at each point both in the internal and external regions. The behavior of the fields on the surface s is rather sensitive to compute, particularly in the proximity of corners, where the transverse tangential components suddenly change directions. Examples of the spatial behaviors of the unknown tangential electric fields at the interface (longitudinal E_z and transverse E_l) are plotted in Fig. 6(a) and (b), respectively, for the first mode of a rectangular cross-section dielectric guide with an

TABLE I
BEM RESULTS FOR THE RESONANCE FREQUENCIES f_{res} OF NRD RECTANGULAR-SECTION RESONATORS OF VARIOUS LENGTHS l, IN THE PEW CASE AS IN FIG. 5(a). REFERENCE DATA ARE DERIVED THROUGH OTHER NUMERICAL TECHNIQUES AND MEASUREMENTS [9]: TRT (TRANSVERSE RESONANCE TECHNIQUE), PMM (POINT MATCHING METHOD), FEM (FINITE ELEMENT METHOD). PARAMETERS: AS IN FIG. 5

fres [GHz] / l [mm]	Measured Values	TRT	PMM	FEM	BEM
10	11.21	11.21	11.18	11.22	11.13
15	10.73	10.72	10.73	10.80	10.72
20	10.50	10.47	10.50	10.54	10.49
25	10.36	10.32	10.30	—	10.34
30	10.23	10.23	—	—	10.24
35	10.17	10.17	—	—	10.17
40	10.13	10.12	—	—	10.13

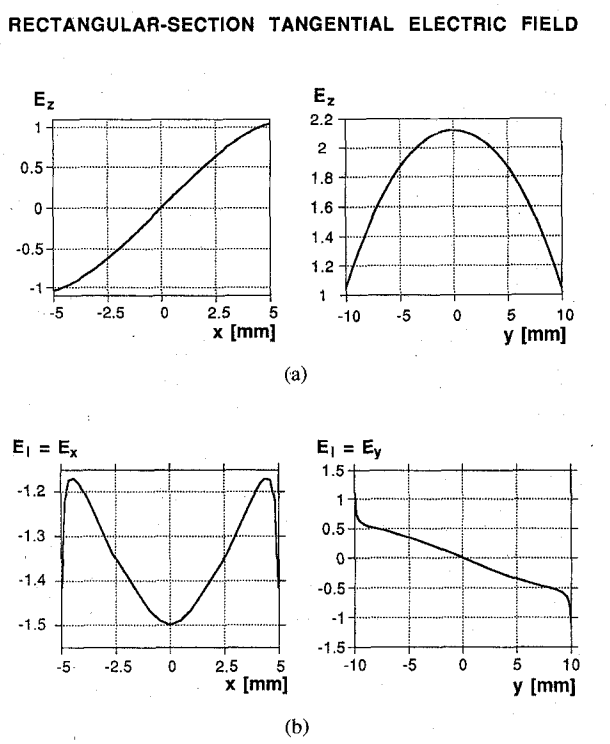

Fig. 6. BEM solutions of the tangential electric field on the air/dielectric interface for the first mode of a rectangular-section dielectric waveguide, with a PEW at $x = 0$ and a PMW at $y = 0$: (a) longitudinal component E_z versus x (left) and versus y (right); (b) transverse component $E_l = E_x$ versus x (left) and $E_l = E_y$ versus y (right). Parameters: $\varepsilon_r = 2.53; b = 10$ mm; $l = 20$ mm; $f = 10.5$ GHz.

$x = 0$ perfect-electric and a $y = 0$ perfect-magnetic symmetry walls.

As a further significant check of the proposed approach, we have also considered dielectric structures with a circular cross section, which has been approximated by a polygon with a sufficiently-large number of sides. Representative examples are reported in Table II for some disc NRD resonators (radius R, height a), giving the frequencies f of the hybrid modes HEM_{npm} in the usual NRD operating range [9] (indices

TABLE II
BEM COMPUTATION OF THE RESONANT FREQUENCIES IN NRD RESONATORS WITH CIRCULAR CROSS SECTION OF RADIUS R AND HEIGHT a; (a) MODES FOR A REXOLITE RESONATOR IN USUAL NRD OPERATING RANGE: THE PERCENTAGE OF ERROR IS CALCULATED WITH RESPECT TO EXACT ANALYTICAL DATA. PARAMETERS: $\varepsilon_r = 2.53$; $R = 11$ mm; $a = 12.3$ mm; (b) MODES FOR A HIGH-PERMITTIVITY PARALLEL-PLATE DIELECTRIC RESONATOR: COMPARISONS ARE PRESENTED WITH REFERENCE TO EXACT VALUES AND TO DATA REPORTED IN TABLE 3.1 OF [15]. PARAMETERS: $\varepsilon_r = 38$; $R = a = 4.25$ mm

Modes HEM npm	BEM Values f[GHz]	Error %
HEM 111	9.225	- 0.03
HEM 011	10.698	0.00
HEM 021	11.137	- 0.01
HEM 211	11.335	- 0.02

(a)

Disc Resonator Modes	f_{res} [GHz] Exact Solutions	f_{res} [GHz] Ref. [15]	f_{res} [GHz] BEM
HEM 111	6.99	7.07	6.98
TE 011	7.98	7.98	7.98
HEM 211	8.73	8.76	8.72
TM 011	8.97	9.21	8.95
HEM 121	9.72	9.77	9.72
HEM 311	10.68	10.90	10.68
HEM 131	11.29	11.46	11.29
HEM 221	11.51	11.80	11.50
HEM 112	12.16	12.13	12.16
TE 021	12.20	12.02	12.20
HEM 411	12.70	12.69	12.70
TE 012	12.96	13.14	12.96
HEM 212	13.23	13.26	13.23

(b)

n, p, m refer to the angular, radial, and axial variations, respectively). The data of Table II(a) are for a rexolite NRD disc resonator for X-band applications. In Table II(b), the results have been simulated for a high-permittivity parallel-plate dielectric resonator of ceramic type ($\varepsilon_r = 38$), for which reference data are also available in the literature [15].

For this circular cross-section geometry, the accuracy of the BEM values has been expressed through a relative error that is evaluated with respect to the results derived by a classical rigorous approach for circular dielectric rods, based on the straightforward solution of the eigenvalue transcendental equation [9], [15]. The agreement between BEM and "exact" results appears in all cases to be remarkable.

The BEM method has also been tested by considering dielectric structures having nonconventional shapes. In particular, slight perturbations in the cross-section geometry have recently found an increasing interest in specific microwave devices: e.g., compact high-performance filters of dual-mode type can be obtained by making use of dielectric resonators with notches or cuts altering their rotational symmetry. The effect of a proper geometrical perturbation on a circular or square resonator is to separate a degenerate modal frequency into a pair of close frequencies ("quasidual" modes) [10].

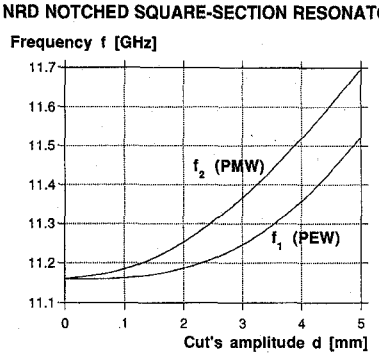

Fig. 7. BEM analysis of slightly-perturbed cross sectional shapes: variation of the quasi-dual resonant frequencies f_1 and f_2 for a square-section NRD resonator (illustrated in Fig. 4(b)) as the amplitude d of the corner's cut varies. Parameters: $\varepsilon_r = 2.53$; $a = 12.3$ mm; $b = 10$ mm.

The accurate prediction of the location of such close resonances as a function of the small perturbations, which is a basic prerequisite for filter design, represents a very difficult task for solution with numerical procedures. The example that has been presented in Fig. 7 refers to a notched square-section NRD resonator, as shown in Fig. 4(b): a symmetric cut of amplitude d is derived along a corner of the square-section parallelepiped (height a, unperturbed sides b, notched sides c, so that $b = c + d$): in this case, the couple of resonances are related to a perfect-electric and to a perfect-magnetic symmetry wall placed along the notched-square minor diagonal, dashed in Fig. 4(b). The BEM approach enables us to precisely calculate the variation of the location of the quasidual resonant frequencies f_1 and f_2 as a function of the perturbation d, as shown in Fig. 7 for the lowest pair of resonances: the larger the notch, the greater the frequency separation. The experimental investigation on such components [10] shows the full agreement with this theoretical behavior.

C. Comments on the Features of the Method

The tests that have been carried out illustrate many favorable properties which make this BEM formulation competitive in comparison with any other numerical technique for obtaining a complete solution of the modal properties in arbitrary dielectric waveguides. Some considerations of the relevant computational features are discussed next.

First, as previously mentioned, this method has demonstrated a very good computing efficiency. The storage requirements depend on the number of points N chosen on the contour for the unknown expansion, so that the zeroing of a determinant corresponding to a $4N \times 4N$ matrix is usually required. Since the convergence of the method is quite fast, accurate solutions may be achieved with limited memory space. As a proof of the effectiveness of the method, representative tests of the convergence properties are given in Table III for the unconventional geometry of a notched square-section NRD resonator: the accuracy in the calculation of the quasidual resonant frequencies is evaluated for different choices of the number of points on the various sides of the contour. It is observed that an excellent numerical stability of

TABLE III

BEM CONVERGENCE PROPERTIES. ACCURACY TESTS OF QUASIDUAL RESONANCE FREQUENCIES f_1 (PEW) AND f_2 (PMW) FOR DIFFERENT CHOICES OF THE NUMBER OF POINTS N_b, N_c, N_d ON THE SIDES b, c, d OF A NOTCHED SQUARE-SECTION NRD RESONATOR· (a) f_1, f_2 VALUES (ROUNDED AT THE MHz) FOR N_b, N_c, N_d VARIABLE IN PROPORTION TO THE LENGTHS OF THE SIDES b, c, d; (b) f_1, f_2 VALUES (ROUNDED AT THE MHz) FOR N_b, N_c, N_d EQUAL FOR ALL THE SIDES. c) PERCENTAGES OF ERROR FOR THE f_1, f_2 VALUES AS THE NUMBER OF POINTS $N_b = N_c = N_d$ INCREASES FURTHER (THESE FREQUENCY VARIATIONS ARE OF THE ORDER OF TENS OF kHz). THE REFERENCE EXACT VALUES ARE THOSE OF THE CASE $N_b = N_c = N_d = 10 : f_1 = 11.1853$ GHz, $f_2 = 11.2528$ GHz. PARAMETERS AS IN FIG. 7; $d = 2$ mm

Side b # points N_b	Side c # points N_c	Side d # points N_d	f_1 [GHz] (PEW)	f_2 [GHz] (PMW)
3	2	1	11.191	11.260
5	4	1	11.188	11.255
6	4	2	11.187	11.253
10	8	2	11.185	11.253

(a)

Side b # points N_b	Side c # points N_c	Side d # points N_d	f_1 [GHz] (PEW)	f_2 [GHz] (PMW)
1	1	1	11.137	11.210
2	2	2	11.190	11.266
3	3	3	11.185	11.255
4	4	4	11.185	11.254
5	5	5	11.185	11.253

(b)

Side b # points N_b	Side c # points N_c	Side d # points N_d	Error % f_1 (PEW)	Error % f_2 (PMW)
6	6	6	0.0027	0.0033
7	7	7	0.0018	0.0015
8	8	8	0.0009	0.0011
9	9	9	0.0004	0.0004

(c)

the solution is generally achieved with a very small number of points.

Furthermore, with the Nystrom method the speed in calculating the matrix elements is particularly high, so that the calculation time is greatly reduced. As an example, for the search of all the solutions for the circular cross-section structure illustrated in Table II(a) (choice of 12 equivalent-polygonal sides with 2 points for each side, in the frequency range 9–11.5 GHz with a step of 50 MHz), a CPU time of about 40 seconds was needed on an HP-712 workstation.

This method is very general in terms of both the characteristics of the media and the geometries of the structures. In fact, it has turned out that our formulation is particularly accurate in modeling any dielectric contour, both those with curved shapes (as for the circular cross section), and those with sharp corners (as for the triangular and notched sections).

Moreover, the accuracy has been demonstrated to be completely adequate to calculate the characteristics of all the modal solutions, for any order of mode (as in the examples of the circular and rectangular resonators) and even in the sensitive situations of nearly degenerate modes (as in the example of the notched resonator). In addition, it should be noted that in all the cases no spurious solution has been generated.

The method works very well in very different frequency ranges, giving satisfactory results both at high frequency and when the cutoff region is approached (see, as an example, the data for the rectangular cross section, and particularly for the image line).

Although a fair amount of analytic pre-processing is required for such a BEM formulation, once the numerical implementation is carried out, the computer program appears rather straightforward and simple to use.

V. CONCLUSION

Even though the boundary element method is in principle a well-known technique for solving efficiently a variety of electromagnetic problems, in practice a great deal of difficulties can arise from a numerical point of view. The BEM procedure that has been developed here allows us to obtain a complete modal characterization of arbitrarily-shaped dielectric waveguiding structures making use of a novel formulation, which considerably improves the computational speed, convergence, and accuracy.

These important advantages have been achieved through an analytical development that allows us to advantageously avoid derivative operations on the unknowns. To reduce the phenomena of numerical instability, a careful theoretical evaluation of singular terms has been performed. The numerical solution has then been carried out by using both standard (method of moments) and alternative methods of discretization.

Specifically, a novel implementation, not applicable to the formulations already presented in the literature (since the absence of derivatives on the unknowns is a prerequisite), was of particular interest: this procedure is based on a proper adaptation of the integral-equation solution method due to Nystrom, and requires neither a choice of basis functions for the unknowns nor any numerical integration on the boundary. Using this method of discretization, the BEM formulation has furnished very fast and precise results, as confirmed by comparisons with reference theoretical and experimental data for various dielectric structures employed in practice.

Even compared to well-known rigorous numerical methods (finite elements, mode matching, etc.), this new BEM formulation has proven to be a very accurate and useful tool for efficient and versatile analysis of a wide variety of waveguiding structures.

ACKNOWLEDGMENT

The authors would like to thank D. Argentieri for useful tests of the Fortran codes, and D. R. Jackson for helpful comments on the manuscript.

REFERENCES

[1] R. E. Collin, *Field Theory of Guided Waves*. New York: IEEE Press, 1991, Ch. 6 and 11.

[2] D. Marcuse, *Theory of Dielectric Optical Waveguides*. Orlando, FL: Academic Press, 1974.

[3] S. M. Saad, "Review of numerical methods for the analysis of arbitrarily-shaped microwave and optical dielectric waveguides," *IEEE Trans. Microwave Theory Tech.*, vol. MTT-33, pp. 894–899, Oct. 1985.
[4] R. Sorrentino, Ed., *Numerical Methods for Passive Microwave and Millimeter Wave Structures*. New York: IEEE Press, 1989, Part 5.
[5] R. E. Collin and D. A. Ksienski, "Boundary element method for dielectric resonators and waveguides," *Radio Sci.*, vol. 22, pp. 1155–1167, Dec. 1987.
[6] N. Morita, N. Kumagai, and J. R. Mautz, *Integral Equation Methods for Electromagnetics*. Norwood, MA: Artech House, 1990, Ch. 2–4.
[7] F. Olyslager and D. De Zutter, "Rigorous boundary integral equation solution for general isotropic and uniaxial anisotropic dielectric waveguides in multilayered media including losses, gain and leakage," *IEEE Trans. Microwave Theory Tech.*, vol. 41, pp. 1385–1392, Aug. 1993.
[8] W. H. Press, S. A. Teukolsky, W. T. Vetterling, and B. P. Flannery, *Numerical Recipes in Fortran*. Cambridge, UK: Cambridge Univ. Press, 1992, Ch. 4 and 18.
[9] F. Frezza, A. Galli, G. Gerosa, and P. Lampariello, "Characterization of resonant and coupling parameters of dielectric resonators for NRD filtering devices," in *MTT-S Int. Microwave Symp. Dig.*, Atlanta, GA, June 1993, pp. 893–896.
[10] C. Di Nallo, F. Frezza, A. Galli, G. Gerosa, M. Guglielmi, and P. Lampariello, "Experimental investigation on NRD-guide dual-mode filters," in *MTT-S Int. Microwave Symp. Dig.*, San Diego, CA, May 1994, pp. 237–240.
[11] K. Solbach and I. Wolff, "The electromagnetic fields and the phase constants of dielectric image lines," *IEEE Trans. Microwave Theory Tech.*, vol. MTT-26, pp. 266–274, Apr. 1978.
[12] E. A. J. Marcatili, "Dielectric rectangular waveguide and directional coupler for integrated optics," *Bell Syst. Tech. J.*, vol. 48, pp. 2071–2102, Sept. 1969.
[13] J. E. Goell, "A circular-harmonic computer analysis of rectangular dielectric waveguides," *Bell Syst. Tech. J.*, vol. 48, pp. 2133–2160, Sept. 1969.
[14] M. Koshiba and K. Inoue, "Simple and efficient finite-element analysis of microwave and optical waveguides," *IEEE Trans. Microwave Theory Tech.*, vol. 40, pp. 371–377, Feb. 1992.
[15] D. Kajfez and P. Guillon, Eds., *Dielectric Resonators*. Norwood, MA: Artech House, 1986, Ch. 3.

Carlo Di Nallo (S'95) received the "laurea" degree cum laude in electronic engineering from "La Sapienza" University of Rome, Italy, in 1992. In 1992, he joined the Electronic Engineering Department of the same university as a doctoral student in applied electromagnetics.

His scientific interests concern mainly electromagnetic theory and applications, involving, in particular, numerical procedures of analysis and synthesis for microwave and millimeter-wave passive components, such as waveguides, resonators, filters, and leaky-wave antennas.

Mr. Di Nallo is a member of SIMAI (Italian Society of Applied and Industrial Mathematics).

Fabrizio Frezza (S'87-M'92) received the "laurea" degree cum laude in electronic engineering from "La Sapienza' University of Rome, Italy, in 1986. In 1991 he obtained the Doctorate in applied electromagnetics from the same university.

In 1986, he joined the Electronic Engineering Department of the same university, where he has been a Researcher since 1990, and a temporary Professor of Electromagnetics since 1994. His main research activity concerns guiding structures, antennas and resonators for microwaves and millimeter waves, numerical methods, scattering, optical propagation, and plasma heating.

Dr. Frezza is a member of Sigma Xi, of AEI (Electrical and Electronic Italian Association), of SIOF (Italian Society of Optics and Photonics), and of SIMAI (Italian Society of Applied and Industrial Mathematics).

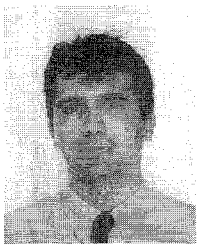

Alessandro Galli (S'91) received the degree in electronic engineering in 1990 and the Doctorate in Applied Electromagnetics in 1994, both from "La Sapienza" University of Rome, Italy.

In 1990, he joined the Electronic Engineering Department of the same university. The main part of his research activity concerns the analysis and design of microwave devices, involving dielectric and anisotropic waveguides and resonators, filters, and leaky-wave antennas; he is also involved in bioelectromagnetics as regards the modeling of interaction mechanisms of electromagnetic fields at cell level.

Dr. Galli is member of the EBEA (European BioElectromagnetics Association). He received the Quality Presentation Recognition (Technical Program Chairman's Honor Roll), granted at the 1994 International Microwave Symposium of MTT-S.